



## MHD Free-Convective Couette flow in a Vertical Porous Microchannel Using Non-Linear Boussinesq Approximation

<sup>1</sup>Samaila K. Ahmad, <sup>2</sup>Basant k. Jha, <sup>2,3</sup>Ayyub M. Hussaini, <sup>2,4</sup>Muhammad M. Altine

<sup>1</sup>Department of Mathematics, Usmanu Danfodiyo University, Sokoto, P.M.B. 2346, Sokoto, Nigeria.

<sup>2</sup>Departement of Mathematics, Ahamadu Bello University, Zaria, Kaduna, P.M.B.1045, Nigeria.

<sup>3</sup>Departement of Mathematics, Shehu Shagari College of Education, Sokoto, P.M.B. 2129, Nigeria.

<sup>4</sup>Departement of Mathematics, Federal University, Birnin Kabbi, Kebbi, P.M.B. 1157 Nigeria.

Email: <sup>1</sup>[ahmadkenga@gmail.com](mailto:ahmadkenga@gmail.com) (+2348036120027), <sup>2</sup>[basant777@yahoo.co.uk](mailto:basant777@yahoo.co.uk)

(+2348027416958), <sup>3</sup>[muhammadavuba90@gmail.com](mailto:muhammadavuba90@gmail.com) (+2348036087890),

<sup>4</sup>[altine@fubk.edu.ng](mailto:altine@fubk.edu.ng) (+2348064819725)

### Abstract

An analytical solution for free convection flow of an electrically conducting fluid in a vertical micro-porous-channel, in the existence of transversely applied magnetic-field and nonlinear Boussinesq approximation is carried out in this article. The governing equations representing stated objective are obtained and solved analytically using method of undetermined coefficients and direct integration. Pictorial and tabular representations of solutions obtained are carried out, so as to ascertain the role of various governing parameters entering flow formation. During the course of numerical simulation of results, it is found that the volumetric flow rate increases with increase in Couette flow parameter, asymmetric heating parameter and suction/injection parameter but decreases with increase in nonlinear Boussinesq approximation parameter.

**Key-words:** Free convection; Microchannel; MHD; nonlinear Boussinesq approximation parameter; Couette flow; Porous channel; Vertical channel.

### 1. Introduction

The free convection flow (also known as natural convection flow) is a mechanism of heat transfer in which flow formation is induced by density difference caused by temperature change. Over the years, this phenomenon has attracted significant application as cooling mechanism for nuclear plants, electronics and micro-chips. Some of the earliest works in the field are the works of Ostrach [1] and Sparrow and Gregg [2]. In these works, they studied the natural convection flow in between two vertical parallel plates with constant temperature and constant heat flux respectively. Since then different works had been

carried-out for better understanding of this phenomenon. Aung [3] and Aung *et al.* [4] respectively examined the fully developed and developing natural convection flow in vertical flat plates with asymmetric heating. Gebhart *et al.* [5] offered extensive review on free-convection flow.

Classifications of flow regime based on the work of Schaaf and Chambre [6] suggested that flows in macro-channel are relatively different from those in micro-channel. In view of this, Chen and Weng [7] extended the work of [3] by considering the role of velocity-slip as well as temperature jump on natural convection flow formation. They resolved that temperature jump

condition induced by the effects of rarefaction and fluid-wall interaction plays an important role in slip-flow natural convection. Flow formations with fluid injection/suction has significant importance in the design of aircrafts and stability of space-ships. Jha *et al.*[8] extended the work of [7] by incorporating fluid injection/suction. They found that that as suction/injection on the channel surfaces increases, the volume flow rate increases and the rate of heat transfer decreases. Other related articles on natural convection flow formations can be seen in ([9], [10], [11], [12]).

Flow formations of electrically conducting fluid are often influence by Lorentz force due to the presence of magnetic field. This concept has been used over the years in power generation and design of magnetohydrodynamics (MHD) generators. Many works have been contributed in this research field. For instance, Jha et al. [13] examined the role of magnetic field on natural convection flow in a microchannel with suction/injection as an extension of [8] in the presence of transversely applied magnetic field. Also, Jha and Oni [14] studied the impact of mode of application of magnetic field on rarefied gas in a microtube. Other related articles include ([15], [16]).

The analysis of nonlinear Boussinesq approximation finds its relevance when the temperature difference between the channel walls is appreciably large. In order to capture a real-life scenario, the nonlinear Boussinesq approximation (NBA) are replaced with the linear Boussinesq approximation (LBA). Goren [17] was the earliest scientist to obtained the condition for using the NBA. Later, Vajravelu and Sastrit[18] analysed the free convection flow between two parallel vertical walls using the combined linear and quadratic density variation with temperature (NDT). They resolved that the presence of NDT leads to an increase in fluid temperature and velocity. Recently, Jha and Oni ([19], [20]) respectively examined the impact of NBA on mixed convection flow in macro vertical and inclined channels. They discovered that the role of NBA parameter is to increase reverse flow formation at the walls and fluid velocity.

The novelty of the current work is the derivation of analytical solutions for MHD natural convection flow in a vertical microchannel with suction/injection and nonlinear Boussinesq approximation. The current work

is the generalization of [13] in the presence of nonlinear Boussinesq approximation and motion of the plate  $y = 0$ .

## Nomenclature

$B_0$	- constant magnetic flux density
$C_p, C_v$	- specific heats at constant pressure and constant volume, respectively
$f_t, f_v$	- thermal and tangential momentum accommodation coefficients, respectively
$In$	- fluid wall interaction parameter
$Kn$	- Knudsen number
$m$	- volume flow rate
$Q$	- dimensionless volume flow rate
$M$	- Hartman number
$Nu$	- Nusselt number
$Pr$	- Prandtl number
$T$	- temperature of fluid
$U$	- dimensionless velocity
Greek letters	
$\alpha$	- thermal diffusivity
$\beta$	- thermal expansion coefficient
$\beta_t, \beta_v$	- dimensionless variables
$\delta$	- Nonlinear Boussinesq approximation parameter (NBA)
$\gamma_s$	- ratio of specific heats
$\mu$	- dynamic viscosity
$\theta$	- dimensionless temperature
$\xi$	- wall ambient temperature difference ratio
$\rho$	- density
$\sigma$	- electrical conductivity of the fluid
Subscripts	
1	- hotter wall values
2	- cooler wall values

## 2. Mathematical Problem

Reconsider the work of Jha *et al.* [13]. The flow is caused by temperature difference at the microchannel walls. Fluid is injected from the wall  $y = b$  and then sucked out at the wall  $y = 0$  for continuity to be satisfied. The microchannel plate  $y = 0$  is assumed to be moving with impulsive velocity in the direction of flow formation as shown in Figure 1. All physical quantities described in this figure are well-defined in nomenclature.

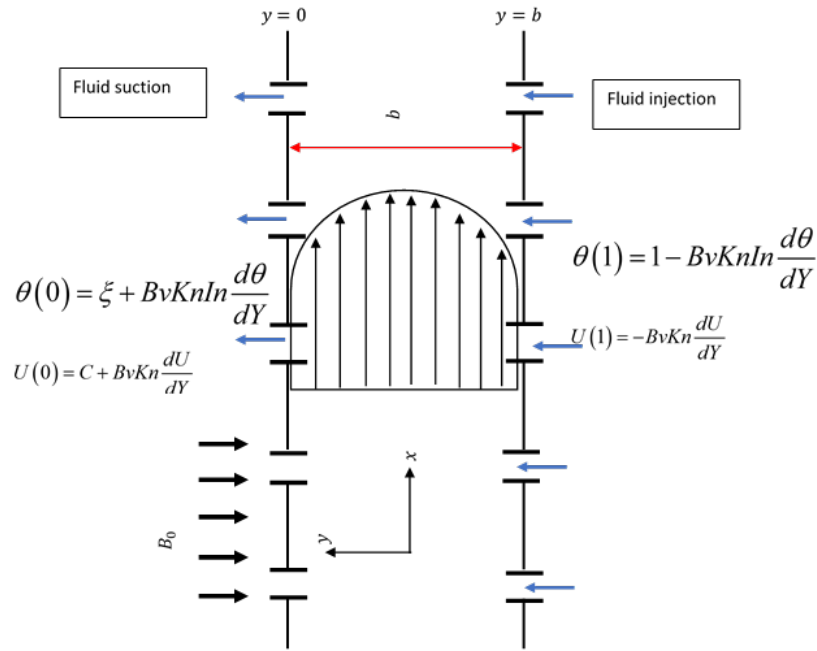


Figure 1: Schematic of flow formation

As a result of Chen and Weng [7] and Jha *et al.*[13] by taking the report of the conducting fluid and rarefaction parameter. The governing equations for the transportation processes in dimensionless form in the presence of velocity slip and temperature jump under nonlinear Boussinesq approximation (NBA) are developed as follows.

$$\frac{d^2U}{dY^2} + S \frac{dU}{dY} - M^2U + \theta + \delta\theta^2 = 0 \quad (1)$$

$$\frac{d^2\theta}{dY^2} + S \text{Pr} \frac{d\theta}{dY} = 0 \quad (2)$$

The dimensionless quantities which are used in the above equations are as follows:

$$X = \frac{x}{b}, Y = \frac{y}{b}, \theta = \frac{T - T_0}{T_1 - T_0}, U = \frac{u}{U_0}, M^2 = \frac{\sigma B_0^2 b^2}{\rho \nu}, \text{Pr} = \frac{\nu}{\alpha}, U_0 = \frac{\rho_0 g \beta (T_1 - T_0) b^2}{\mu},$$

$$S = \frac{V_0 b}{\nu} \text{ and } \delta = \frac{\beta_1}{\beta_0} (T_1 - T_0) \quad (3)$$

The boundary conditions which express the velocity slip and temperature jump conditions at the fluid wall interface are as follows:

$$U(0) = C + BvKn \frac{dU}{dY}, \quad \theta(0) = \xi + BvKn \ln \frac{d\theta}{dY} \quad \text{at } Y = 0$$

$$U(1) = -BvKn \frac{dU}{dY}, \quad \theta(1) = 1 - BvKn \ln \frac{d\theta}{dY} \quad \text{at } Y = 1 \quad (4)$$

The dimensionless quantities for the boundary conditions are as follows:

$$B_v = \frac{2 - f_v}{f_v}, \quad B_t = \frac{2 - f_t}{f_t} \frac{2\gamma_s}{\gamma_s + 1} \frac{1}{\text{Pr}}, \quad Kn = \frac{\lambda}{b}, \quad In = \frac{B_t}{B_v}, \quad \xi = \frac{T_2 - T_0}{T_1 - T_0}, \quad \text{and } C = \frac{u}{U_0}$$

Equations (1) and (2) subject to the boundary conditions (4) have the following exact solutions:

$$\theta(Y) = B_1 e^{-SPr} + B_2 \quad (5)$$

$$U(Y) = B_3 e^{\lambda_1 y} + B_4 e^{-\lambda_2 y} + B_5 e^{-2SPr} + B_6 e^{-SPr} + B_7 \quad (6)$$

where:

$$B_1 = \frac{B_{13}}{B_{15}}, B_2 = \xi - \frac{B_{13} B_{14}}{B_{15}}, B_3 = \frac{B_{10} - B_4 B_{18}}{B_{19}}, B_4 = \frac{-(B_{19}(B_{11} + B_{12} BvKn) + B_{10} B_{20} e^{\lambda_1})}{(B_{19} B_{21} e^{-\lambda_2} - B_{18} B_{20} e^{\lambda_1})}, B_5 = \frac{-\delta B_1^2}{B_{16}},$$

$$B_6 = \frac{-(B_1 + 2\delta B_1 B_2)}{B_{17}}, B_7 = \frac{(B_2 + \delta(B_2)^2)}{m^2}, B_8 = B_5 + B_6 + B_7, B_9 = -2B_5 SPr - B_6 SPr,$$

$$B_{10} = C + B_9 BvKn - B_8,$$

$$B_{11} = B_5 e^{-2SPr} + B_6 e^{-SPr} + B_7 \text{ and } B_{12} = -2B_5 SPr e^{-2SPr} - B_6 SPr e^{-SPr}$$

The important parameter for buoyancy induced micro-flow is the volumetric flow-rate  $Q$ . The dimensionless volumetric flow-rate is:

$$Q = \frac{m}{bU_0} = \int_0^1 U dY \quad (7)$$

Substituting equation (6) into equation (7) we got

$$Q = \frac{B_3}{\lambda_1} (e^{\lambda_1} - 1) - \frac{B_4}{\lambda_2} (e^{-\lambda_2} - 1) - \frac{B_5}{2SPr} (e^{-2SPr} - 1) - \frac{B_6}{SPr} (e^{-SPr} - 1) + B_7 \quad (8)$$

To obtain the skin friction ( $\tau$ ) on the micro channel vertical plates, we differentiated expression (6) with respect to  $Y$  as follows:

$$\tau_0 = \lambda_1 B_3 - \lambda_2 B_4 2SPr B_5 - SPr B_6 \quad (9)$$

$$\tau_1 = \lambda_1 B_3 e^{\lambda_1} - \lambda_2 B_4 e^{-\lambda_2} - 2SPr B_5 e^{-2SPr} - SPr B_6 e^{-SPr} \quad (10)$$

Where:

$$B_{13} = 1 - \xi, B_{14} = (1 + SPr BvKn \ln), B_{15} = (e^{-SPr} - SPr BvKn \ln(e^{-SPr} + 1) - 1),$$

$$B_{16} = (2SPr)^2 - 2S^2 Pr - m^2, B_{17} = (SPr)^2 - S^2 Pr - m^2, B_{18} = (1 + \lambda_2 BvKn), B_{19} = (1 - \lambda_1 BvKn),$$

$$B_{20} = (1 + \lambda_1 BvKn), B_{21} = (1 - \lambda_2 BvKn), \lambda_1 = \frac{-S + \sqrt{S^2 + 4m^2}}{2} \text{ and } \lambda_2 = \frac{-S - \sqrt{S^2 + 4m^2}}{2}.$$

### 3. Results and Discussion

An analytical solution for free convection flow of an electrically conducting fluid in a vertical micro-porous-channel in the presence of transversely applied magnetic field and nonlinear Boussinesq approximation is carried out in this article. The closed-form solutions obtained signifies that fluid temperature, velocity, skin-friction and volumetric

flow rate are controlled by the Prandtl number ( $Pr$ ), suction/injection parameter ( $S$ ), wall ambient temperature difference ratio ( $\xi$ ), Couette flow parameter ( $C$ ) and nonlinear Boussinesq approximation ( $\delta$ ). For proper understanding of the role of these parameters, graphs are plotted for fluid temperature and velocity, while tabular analysis are carried out for skin-frictions at the microchannel wall and volumetric flow rate in the microchannel.

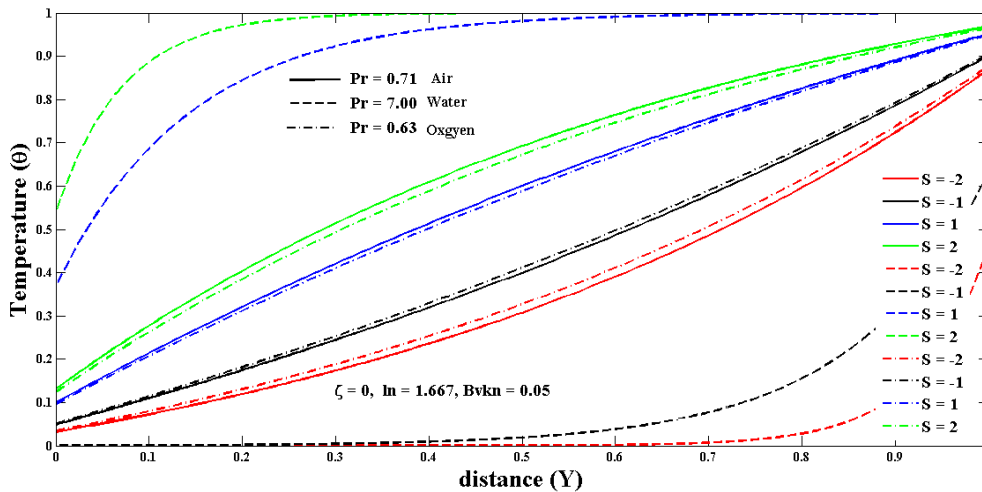


Figure 2: Temperature distributions for different values of  $Pr$  and  $S$

Figure 2 presents the temperature distributions as a function of Prandtl number and suction/injection parameter. From this figure, it is found that fluid temperature increases with increase  $Pr$  and injection parameter ( $S$ ) regardless of the fluid considered. This could be attributed to the fact that, negative values of  $S$  signifies that fluid is being injected from the wall  $Y = 0$  and sucked out at  $Y = 1$ , which inturns leads to decline in fluid temperature, regardless of the working fluid. A relook at this figure also indicates that the maximum temperature is achieved for water ( $Pr = 7.0$ ), and this could be attributed to the high viscosity of water, relative to air or oxygen.

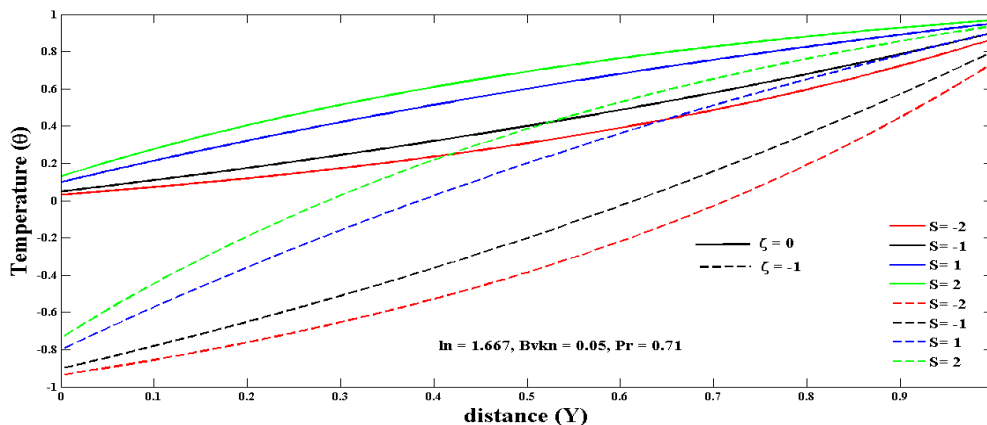


Figure 3: Temperature distributions for different values of  $\zeta$  and  $S$ .

Figure 3 in similar trend establishes the combined effect of wall ambient temperature difference ratio and suction/injection parameter on fluid temeprature in the microchannel. This result shows an upward trend in fluid temperature as you proceed along the microchannel ( $Y = 0$  to  $Y = 1$ ). Infact, it is found that that maximum temperature canbe achieved when fluid boundary conditions are asymmetric in nature. This could be attributed to the fact that temperature increases when both walls are heated symmetrically, or one wall is heated, while the other is kept at room temperature relative to the case  $\zeta = -1$ , where the microchannel wall  $Y = 0$  is cooled.

Figure 4 depicts velocity profile for different values of nonlinear Boussinesq approximation parameter and Couette flow parameter. It is obvious from this figure that fluid velocity increases in the presence of motion of the plate  $Y = 0$  ( $C = 1$ ), relative to the static case ( $C = 0$ ) regardless of the value of  $\delta$ . Also, it is observed that fluid velocity for LBA are greater than those of NBA. This finding demonstrated that fluid velocity could have been overestimated, if the NBA had not been put into consideration.

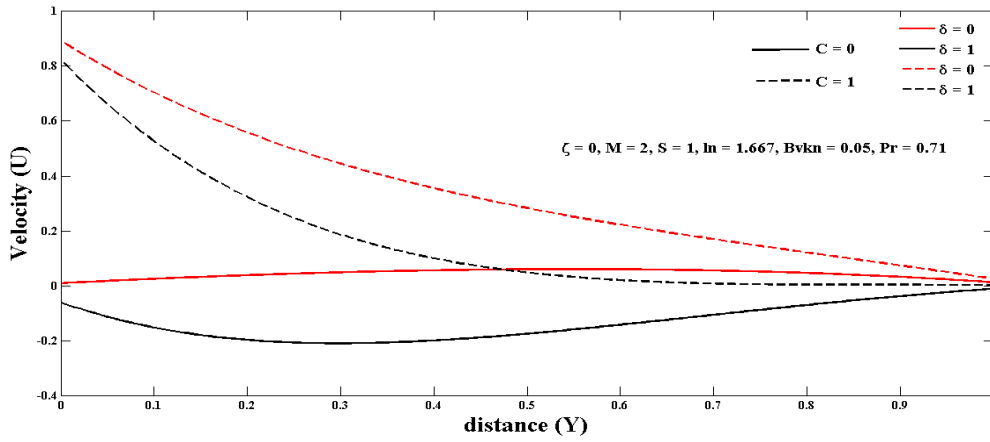


Figure 4: Velocity profile for different values of nonlinear Boussinesq approximation parameter and Couette flow parameter.

Figure 5 portrays the velocity profile in the microchannel as a function of suction/injection parameter ( $S$ ) and Couette flow parameter ( $C$ ). It is detected from this figure that velocity increases with increase in suction and the presence of Couette flow ( $C = 1$ ). This could be explained from the fact that  $C = 1$  implies the plate is moving in direction of flow formation, which then assist fluid velocity along this direction. Figure 6 explains the combined role of suction/injection parameter ( $S$ ) and nonlinear Boussinesq approximation ( $\delta$ ) on velocity profile in the vertical microchannel. This figure clearly demonstrated that the role of NBA is to reduce fluid velocity, regardless of the magnitude of suction/injection parameter.

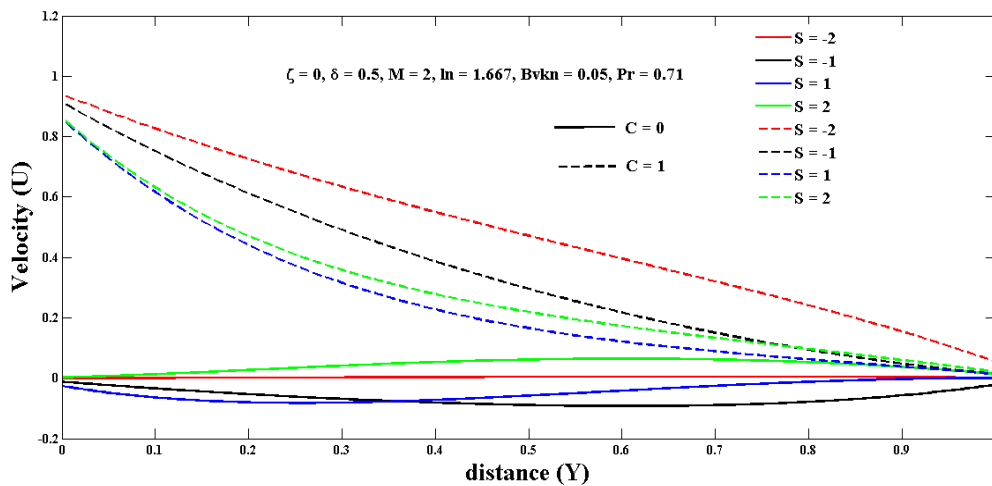


Figure 5: Velocity profile for different values of suction/injection parameter and Couette flow parameter.

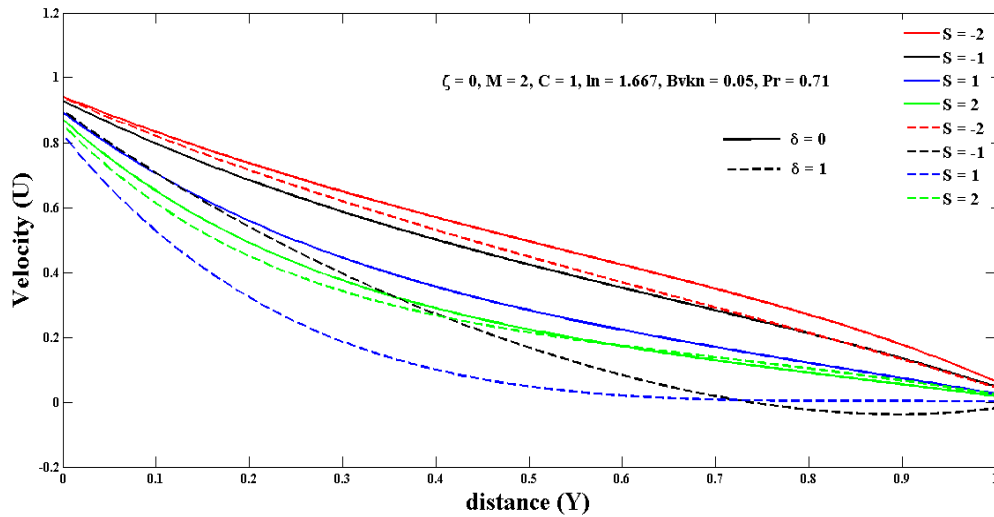


Figure 6: Velocity profile for different values of suction/injection parameter and nonlinear Boussinesq approximation.

Tables 1-3 compute the skin-friction at the microchannel walls functions of Couette flow parameter, suction/injection parameter and nonlinear Boussinesq approximation for purely asymmetric wall heating ( $\xi = 0$ ). It is found from Table 1 that skin-frictions at both microchannel walls decreases in the presence of Couette flow parameter, but increases with increase in fluid injections.

Table 2 on the other hand carried out the same analysis as that of Table 1 for symmetric heating of the wall  $Y = 0 (\xi = 1)$ . This analysis shows similar trend with that of Table 1, but with increase in skin-friction at the walls, which could be attributed to the symmetric nature of wall heating.

Table 1: Shows the Skin friction ( $\tau_0$ ) and ( $\tau_1$ ) for different values of  $\delta$  and  $S$  where  $M = 2$ ,  $B_v kn = 0.05$ ,  $In = 1.667$ ,  $Pr = 0.71$  at  $\xi = 0$ .

$\delta$	$S$	$\tau_0$ at $C = 0$	$\tau_0$ at $C = 1$	$\tau_1$ at $C = 0$	$\tau_1$ at $C = 1$
<b>0.0</b>	1.0	0.1718	-2.1418	-0.2339	-0.4984
	1.5	0.2012	-2.3576	-0.2287	-0.4253
	2.0	0.2311	-2.5844	-0.2214	-0.3650
<b>0.5</b>	1.0	-0.5213	-2.8350	-6.1593e-004	-0.2651
	1.5	-0.1208	-2.6796	-0.2124	-0.4090
	2.0	0.0601	-2.7554	-0.2698	-0.4134
<b>1.0</b>	1.0	-1.2145	-3.5281	0.2327	-0.0319
	1.5	-0.4428	-3.0016	-0.1960	-0.3926
	2.0	-0.1109	-2.9263	-0.3181	-0.4617

For the third case, Table 3 presents same analysis as those of Tables 1 and 2 for the case when that wall  $Y = 0$  is being cooled ( $\xi = -1$ ). The findings in this tables shows that this case has the least skin-frictions at both walls. This could be attributed to the retarded velocity caused by this phenomenon, which then decreases skin-frictions at both walls.

Table 2: Skin friction ( $\tau_0$ ) and ( $\tau_1$ ) for different values of  $\delta$  and  $S$  where  $M = 2$ ,  $B_v kn = 0.05$ ,  $In = 1.667$ ,  $Pr = 0.71$  at  $\xi = 1$ .

$\delta$	$S$	$\tau_0$ at $C = 0$	$\tau_0$ at $C = 1$	$\tau_1$ at $C = 0$	$\tau_1$ at $C = 1$
<b>0.0</b>	1.0	0.3987	-1.9150	-0.3079	-0.5724
	1.5	0.4194	-2.1394	-0.2856	-0.4822
	2.0	0.4386	-2.3768	-0.2643	-0.4079
<b>0.5</b>	1.0	0.5980	-1.7156	-0.4618	-0.7263
	1.5	0.6292	-1.9297	-0.4284	-0.6250
	2.0	0.6579	-2.1575	-0.3965	-0.5401
<b>1.0</b>	1.0	0.7973	-1.5163	-0.6157	-0.8802
	1.5	0.8389	-1.7200	-0.5712	-0.7678
	2.0	0.8773	-1.9382	-0.5287	-0.6723

Table 3: Skin friction ( $\tau_0$ ) and ( $\tau_1$ ) for different values of  $\delta$  and  $S$  where  $M = 2$ ,  $B_v kn = 0.05$ ,  $ln = 1.667$ ,  $Pr = 0.71$  at  $\xi = -1$ .

$\delta$	$S$	$\tau_0$ at $C = 0$	$\tau_0$ at $C = 1$	$\tau_1$ at $C = 0$	$\tau_1$ at $C = 1$
<b>0.0</b>	1.0	-0.0551	-2.3687	-0.1599	-0.4244
	1.5	-0.0170	-2.5758	-0.1718	-0.3684
	2.0	0.0235	-2.7919	-0.1785	-0.3221
<b>0.5</b>	1.0	-2.9719	-5.2855	1.0870	0.8225
	1.5	-1.4977	-4.0565	0.2082	0.0116
	2.0	-0.9032	-3.7187	-0.0612	-0.2048
<b>1.0</b>	1.0	-5.8888	-8.2024	2.3339	2.0694
	1.5	-2.9784	-5.5373	0.5883	0.3917
	2.0	-1.8299	-4.6454	0.0562	-0.0874

Table 4 discusses the combined role of Couette flow parameter, suction/injection parameter and nonlinear Boussinesq approximation for different physical situations ( $\xi = 1, 0, -1$ ) on volumetric flow rate in the vertical microchannel. This table clearly explains that flow rate increases with increase in Couette flow parameter ( $C$ ), asymmetric heating parameter ( $\xi$ ) and suction/injection parameter ( $S$ ) but decreases with increase in nonlinear Boussinesq approximation parameter. Infact, the maximum flow rate is found for the case of symmetric heating. This could be credited to the saturation of heat in the entire microchannel, which inturns increases the amount of fluid passing through the microchannel.

Table 4: Volume flow rate  $Q$  for different values of  $\delta$  and  $S$  where  $M = 2$ ,  $B_v kn = 0.05$ ,  $ln = 1.667$  and  $Pr = 0.71$ .

$\delta$	$S$	$\xi = 0$		$\xi = 1$		$\xi = -1$	
		$Q$ at $C = 0$	$Q$ at $C = 1$	$Q$ at $C = 0$	$Q$ at $C = 1$	$Q$ at $C = 0$	$Q$ at $C = 1$

<b>0.0</b>	1.0	0.0432	0.3377	0.0722	0.3667	0.0141	0.3086
	1.5	0.0458	0.3131	0.0712	0.3385	0.0204	0.2877
	2.0	0.0480	0.2900	0.0699	0.3118	0.0261	0.2681
<b>0.5</b>	1.0	-0.0457	0.2488	0.1084	0.4029	-0.3914	-0.0969
	1.5	0.0178	0.2850	0.1069	0.3741	-0.1477	0.1195
	2.0	0.0422	0.2841	0.1048	0.3468	-0.0583	0.1836
<b>1.0</b>	1.0	-0.1345	0.1600	0.1445	0.4390	-0.7969	-0.5024
	1.5	-0.0102	0.2570	0.1425	0.4097	-0.3158	-0.0486
	2.0	0.0363	0.2783	0.1398	0.3817	-0.1427	0.0992

#### 4. Conclusion

Fluid temperature increases with increase in suction/injection parameter while velocity decreases. Fluid velocity is enhanced in the presence of Couette flow, but retarded in the existence of nonlinear Boussinesq approximation. Frictions at both walls increase as suction/injection parameter and degree of

wall asymmetric parameter increase, but reduce as Couette flow parameter, linear Boussinesq approximation increase. Volumetric flow rate increases with increase in Couette flow parameter, asymmetric heating parameter and suction/injection parameter but decreases with increase in nonlinear Boussinesq approximation parameter.

#### References

- [1] S. Ostrach, "Laminar natural convection flow and heat transfer of fluids with and without heat sources in channels with constant wall temperatures," *NACA TN*, (1952) 2863.
- [2] R. Sparrow and J. Gregg, "Laminar free convection from a vertical plate with uniform surface heat flux," *Trans. Am. Soc. Mech. Engrs.*, (78)1956, 435-440.
- [3] W. Aung, "Fully developed laminar free convection between vertical plates," *Int. J. Heat Mass Transfer*, (15)1972,1577-1580.
- [4] W. Aung, L. Fletcher and V. Sernas, "Developing laminar free convection between vertical plates with asymmetric heating," *Int. J. Heat Mass Transfer*, (15)1972, 2293-2308.
- [5] B. Gebhart, Y. Jaluria, R. L. Mahajan and B. Sammakia, "Buoyancy-induced flows and transport," in *Chapter 14*, New-York, 1988.
- [6] S. Schaaf and P. Chambre, *Flow of Rarefied Gases*, Princeton: Princeton University Press, 1961.
- [7] C. Chen and H. Weng, "Natural convection in a vertical microchannel.," *ASME J. Heat Transfer*, (127)2005, 1053-1056.
- [8] B. K. Jha, B. Aina and S. B. Joseph, "Natural Convection Flow in a Vertical Micro-Channel with Suction/Injection," *Journal of Process Mechanical Engineering*, 228, (3)2014, 171-180.
- [9] B.K. Jha and M.O. Oni, "Transient natural convection flow between vertical concentric cylinders heated/cooled asymmetrically.," *Proc IMechE Part A: Journal of Power and Energy*, 232 (3)2018, 926-939.
- [10] E. Arkilic, K. Breuer and M. Schmidt, "Gaseous flow in microchannels, application of micro-fabrication to fluid mechanics," *ASME FED*, (197)1994, 57-66.
- [11] J. Bodoia and J. Osterle, "The development of free convection between heated vertical plates," *J. Heat Transfer*, vol. 84, pp. 40-44, 1962.

- [12] W. Elenbaas, "Heat dissipation of parallel plates by free convection," *Physica*, (9)1942, 1-28.
- [13] B.K. Jha, B. Aina and A.T. Ajiya, "Role of Suction/Injection on MHD Natural," *International Journal of Energy and Technology*,(7)2015, 30-39.
- [14] B. K. Jha and M.O. Oni, "Impact of mode of application of magnetic field on rate of heat transfer of rarefied gas flow in a microtube," *Alexandria Engineering Journal*, 57(3) 2017, 1955-1962.
- [15] B.K. Jha, L.T. Azeez and M.O. Oni, "Unsteady hydromagnetic-free convection flow with suction/injection," *Journal of Taibah University for Science*, 13(1) 2019, 136-145.
- [16] B. K. Jha and M.O. Oni, "Role of magnetic field on mixed convective flow between two concentric microtubes with heat generation/absorption: An exact solution," *Journal on Nanomaterial Nanoengineering and Nanosystems*,(2018) 1-9.
- [17] S. Goren, " On free convection in water at  $4^{\circ}C$ ," *Chemical and Engineering Science* , (21)1966, 515-518.
- [18] K. Vajravelu and K. Sastrit, "Fully developed free convection flow between two parallel vertical walls-I," *Int. J. Heat and Mass Trans.* , 20 ( 5) 1977 655-660 .
- [19] B.K. Jha and M.O. Oni, "Theory of fully developed mixed convection including flow reversal: A nonlinear Boussinesq Approximation Approach.," *Heat Transfer—Asian Res.*, (2019) 1-12.
- [20] B.K. Jha and M.O. Oni, "Nonlinear Mixed Convection Flow in an Inclined Channel with Time-Periodic Boundary Conditions.," *Int. J. Appl. Comput. Mat.*, (6) 2020, 129.